



Research Paper

Phage display screening for highly specific nickel- and cobalt-binding peptides for bio-recovery of metals

Anna Sieber^a, Anastasia Kalampaka^b, Sabine Matys^c, Franziska Lederer^c,
Klemens Kremser^b, Doris Ribitsch^{b,d,*}, Georg M. Guebitz^{b,d}

^a K1-MET GmbH, Linz, Austria

^b Institute of Environmental Biotechnology, Department of Agricultural Sciences, BOKU University, Tulln an Der Donau, Austria

^c Biotechnology Department, Helmholtz Institute Freiberg for Resource Technology, Helmholtz-Zentrum Dresden-Rossendorf, Dresden, Germany

^d Austrian Centre of Industrial Biotechnology, Tulln an Der Donau, Austria



ARTICLE INFO

Keywords:

Metal-binding peptides
Phage surface display
Biosorption
Isothermal titration calorimetry
Nickel
Cobalt
Electronic waste

ABSTRACT

Electronic waste is a valuable source of critical metals like nickel and cobalt, but their recovery is challenging. Current recycling processes use harsh conditions and toxic chemicals, which is why environmentally friendly alternatives are crucial. Metal-binding peptides offer high selectivity and durability, making them promising for sustainable metal separation. Here, phage display was successfully applied to screen a combinatorial peptide library with specific affinities to nickel or cobalt. Identified peptides with the amino acid sequences FWPLHHH, GPHKHHA, HNYHHRH, and HMNHHHH revealed improved binding affinities of up to 20.000-fold to immobilized metal ions compared to the unspecific binding of the phage backbone. Furthermore, low micromolar dissociation constants e.g., 6.2 μM for peptide Co_02 (HMNHHHH) to Co^{2+} and 29.0 μM for peptide Ni_01 (GPHKHHA) to Ni^{2+} , determined by Isothermal Titration Calorimetry (ITC) measurements confirmed the intrinsic metal binding properties. These peptides offer a high potential for future recycling of nickel and cobalt from mixed metal waste like batteries.

1. Introduction

The enormous electrification of today's society and the transition to electricity from renewable energy increases the demand of critical raw materials. At the same time, e-waste is the highest-growing municipal waste category worldwide and predicted to increase to 74.7 million tons by 2030 (Chakankar et al., 2024; Pommeret et al., 2022). Yet, this e-waste is rich in valuable metals such as Cu, Fe, Ni, Co, Au, Ag, Al, and various rare earth elements to name only a few and is consequently an attractive secondary resource. Recycling of e-waste and valorization of critical and economically important metals is indispensable and will help closing the gap between supply and demand of critical raw materials. However, only a small amount of electronic waste is currently recycled. State-of-the-art recycling approaches rely on pyro- and hydrometallurgical processes. Chemical or biological hydrometallurgical approaches transform the metals into their ionic state either by the application of chemicals or microbes and their metabolic side products. Thereby metals become soluble in aqueous solutions. Current metal

recovery and separation methods from leachates or liquid wastes include selective precipitation, chemical reduction processes, ion exchange, membrane separation or electrolysis (Chakankar et al., 2024; Ye et al., 2024). Ion exchange provides high selectivity for metal ions and simple maintenance but also involves high operational costs (e.g. because of the poor stability of the exchange resin material) and the generation of a concentrated brine waste solution (Chen et al., 2022). Membrane separation operations are more cost effective but can suffer from membrane fouling and poor operational stability e.g. due to solvent loss. Fouling can also occur at the electrode of an electrochemical process, in addition to high energy consumption (Ye et al., 2024). Another major challenge in the beforementioned processes is the efficient separation of transition metal ions such as cobalt, nickel or manganese. Due to their proximity in the periodic table and their frequent occurrence together in nature, they share similar chemical properties making their separation notoriously difficult (Fan et al., 2020; Schaeffer et al., 2020). The coordination chemistry of nickel and cobalt in solution is highly influenced by the solvation environment. In a purely aqueous

* Corresponding author.

E-mail addresses: anna.sieber@k1-met.com (A. Sieber), anastasia.kalampaka@boku.ac.at (A. Kalampaka), s.matys@hzdr.de (S. Matys), f.lederer@hzdr.de (F. Lederer), klemens.kremser@omv.com (K. Kremser), doris.ribitsch@boku.ac.at (D. Ribitsch), guebitz@boku.ac.at (G.M. Guebitz).

<https://doi.org/10.1016/j.wasman.2025.115145>

Received 10 May 2025; Received in revised form 7 July 2025; Accepted 18 September 2025

Available online 22 September 2025

0956-053X/© 2025 The Author(s). Published by Elsevier Ltd. This is an open access article under the CC BY license (<http://creativecommons.org/licenses/by/4.0/>).

environment, both metal ions are stabilized as metal cations forming octahedral complexes where six water molecules coordinate around the metal center. The strong ion–dipole interactions between the metal cations and surrounding water molecules yield $\text{Ni}(\text{H}_2\text{O})_6^{2+}$ and $\text{Co}(\text{H}_2\text{O})_6^{2+}$ as the primary species (Aberdeen et al., 2025). Hydrolysis of $\text{Ni}(\text{H}_2\text{O})_6^{2+}$ to $\text{Ni}(\text{OH})_2$ is not expected at a pH below 8. Similarly, the $\text{Co}(\text{H}_2\text{O})_6^{2+}$ cation can undergo hydrolysis at pH values between 4 and 8 but the hydrolysis species will be approximately two to six orders of magnitude lower than the $\text{Co}(\text{H}_2\text{O})_6^{2+}$ species (Collins & Kinsela, 2010; Hummel & Curti, 2003). In an organic phase, the formation of a tetrahedrally coordinated cobalt species is more favorable than the octahedrally coordinated nickel species (Sole, 2018). Hence, solvent extraction can be used to separate cobalt from nickel and researchers focus on optimizing the selective extractants and making the process more environmentally friendly by switching from highly hazardous organic solvents to green extractants (Chen et al., 2022; El Ouardi et al., 2023). In contrast, applying a biotechnological approach to extract metals from leachates or liquid waste allows for ambient temperatures with lower energy requirement and environmental impact than current approaches (Urbina et al., 2019).

Nature offers a broad toolbox of highly specific biomolecules that can interact with certain metal ions. In fact, 38 % of the entries in the Protein Data Base PDB (Andreini & Rosato, 2022) contain at least one metal ion and it has been estimated that no less than 40 % of enzymes require metal ions for their biological function. The so-called metalloproteins harbor specific binding sites for their target metal ions (Lin et al., 2024). The affinity and selectivity are mainly determined by the properties and sequence of the single amino acids and by the protein/peptide structure. Proteins and peptides share the same amino acid building blocks. However, in contrast to proteins, peptides can be easily equipped with a range of modifications that enable the specific binding to target molecules with high affinity and selectivity. Due to their simpler structure, peptides can retain their functionality within toxic environments and withstand changes in pH and temperature. Depending on the complexity of these peptides they can be produced chemically through solid-phase peptide synthesis or biologically by heterologous expression at relatively low cost. Additionally, peptides demonstrate fast adsorption kinetics with low energy and chemical inputs, therefore offering promising alternatives to traditional metal recovery technologies (Leone et al., 2024; Sosnowska et al., 2025; Techert et al., 2025; Ye et al., 2024).

Taking inspiration from nature, the potential of metal-binding peptides in biosorption processes and biomining technologies was increasingly recognized in the last decade. The application of metal-binding peptides offers effective solutions to extract metals from secondary raw material waste or wastewaters (Sieber et al., 2024). Promising peptides have been identified and applied for the recovery of Cu^{2+} (Sosnowska et al., 2025; Urbina et al., 2019), Li^+ (Jeong et al., 2024; Selvamani et al., 2023), Ni^{2+} and Co^{2+} (Matys et al., 2020, 2022), Ga^{3+} (Schönberger et al., 2021) or rare earth elements (Lederer et al., 2016; Maass et al., 2024) from secondary resources such as electronic waste, battery waste solutions or other contaminated wastewater.

Cutting-edge approaches in rational design, homology modeling or proteomics allow the development of metal-binding peptides, which can further be engineered for improved functionality or other desirable properties. In addition, phage surface display has been shown to be an effective approach for the identification of metal-binding peptides (Chakankar et al., 2024; Ye et al., 2024). Since its discovery in 1985, phage display technology has been implemented in a variety of research fields such as protein engineering, immunology, drug discovery and biotechnology and more recently in environmental remediation including resource recovery (Braun et al., 2018; Sieber et al., 2024; Sosnowska et al., 2025). Applying this method, a plethora of different peptides can be easily screened as part of a peptide library in laboratory conditions to identify promising metal-binding candidates. The most common peptide libraries used to date are based on the M13 phage with modified minor (pIII) or major (pVIII) coat proteins. Biopanning is an

affinity-selection method where those libraries are brought into contact with the target materials, e.g., mineral particles or immobilized metal ions. Following several washing steps to remove weak binders, the binding phages are eluted in an iterative process of up to six rounds under increasingly stringent conditions (Matys et al., 2020).

Biopanning results are prone to be affected by false positive or target unrelated peptides (TUPs). Several researchers have identified TUPs in their enriched peptide sequences not because of their specific binding to the target but because the phage clones were propagating faster during amplification or because of background binding to some constituents of the biopanning setup such as plastic, capturing agents or other contaminants. It is important to clean biopanning results from any false positive results related to TUPs (He et al., 2016; Matochko et al., 2014; Thota et al., 2024). Hence, the development of specific databases for phage display data such as the biopanning data bank (BDB, <https://i.uestc.edu.cn/bdb/>) and related bioinformatic analysis tools e.g., the ones collected in the web tool SAROTUP have gained importance (Huang et al., 2010, Huang et al., 2012).

Using different phage display libraries, various promising peptide candidates binding to different inorganic materials such as the rare earth elements lanthanum phosphate (Lederer et al., 2019) or yttrium oxide (Maass et al., 2024), chromium (Yang et al., 2015) or zinc (Zhang et al., 2019) to name a few have been identified. One step further, researchers have applied these peptides in waste-based biorefinery approaches. For example, Li et al. (2019) displayed nickel-binding peptides on the surface of *Saccharomyces cerevisiae* and confirmed the enhanced biosorptive capacity of the organism for nickel by roughly 80 % (Li et al., 2019). Additionally, gallium-binding peptides were identified in an innovative chromatopanning approach, immobilized on polystyrene beads, and used for the recovery of gallium from process water from a wafer manufacturer (Schönberger et al., 2019, 2021).

For the development of a green recycling technology for lithium-ion batteries, the separation of the two economically significant and chemically similar metal ions nickel and cobalt is of particular interest. Here, specific nickel- and cobalt-binding peptides can play a significant role. In earlier studies, we have identified promising nickel- and cobalt-binding peptides from a constrained heptapeptide library, and their binding strength and selectivity was characterized. The described nickel-binding peptide showed moderate but selective binding to nickel. In contrast, the cobalt-binding peptide, albeit displaying high affinity to cobalt, interacts as well with nickel at nearly identical affinity (Matys et al., 2020, 2022). These results underline the challenging nature of developing highly selective metal-binding peptides and there is still a strong need to improve biopanning procedures to yield more selective binders. In our previous approach, the defined peptide structure given by the screened C7C phage peptide library limits the peptide flexibility due to the formation of disulfide bonds and might thus prevent the formation of a proper metal-binding scaffold.

In this study, affinity-selection was successfully based on a linear heptapeptide phage library and immobilized nickel and cobalt-ions on NTA-agarose beads as target material. Furthermore, the affinity of four selected peptides to their target metal was assessed in single-clone binding tests. For future metal recovery applications, the peptides will be used without the phage backbone. Hence, the four selected peptides were chemically synthesized, and their metal-binding properties and specificity of binding were assessed in isothermal titration calorimetry experiments.

2. Materials and methods

2.1. Materials

Chemicals of analytical grade were purchased from Sigma-Aldrich (Sigma-Aldrich, Austria) unless otherwise specified. For pH measurements, a Mettler Toledo S220 pH-meter with a combined glass electrode (Mettler-Toledo GmbH, Austria) was used. TBS buffer (50 mM Tris-HCl,

150 mM NaCl, pH 7.5) was supplemented with 0.05 % Tween®20 (TBST) for the first two rounds of biopanning. In the third round, the Tween®20 concentration was elevated to 0.1 % to increase the stringency. Centrifugation was performed with either an Eppendorf centrifuge 5417R or 5920R (Eppendorf SE, Germany). Tubes and deep well plates were incubated at 22 °C and 37 °C in an Eppendorf thermomixer Comfort (Eppendorf SE, Germany).

The Ph.D.TM-7 Phage Display Peptide Library Kit v2 (lot number: 10163099) was purchased from NEB (New England Biolabs GmbH, Germany). The heptapeptides from this library are fused via a GGGG linker sequence to the N-terminus of the minor pIII coat protein of M13 phage. The kit included the *Escherichia coli* K12 ER2738 host strain from which a glycerol stock was prepared. This *E. coli* strain was used for the amplification of eluted bacteriophages and for the determination of phage titer. From the glycerol stock, the strain was plated onto LB agar plates (10 g l⁻¹ tryptone, 5 g l⁻¹ yeast extract, 5 g l⁻¹ NaCl and 15 g l⁻¹ agar supplemented with 20 µg ml⁻¹ tetracycline) and maintained during the experiments. LB media (10 g l⁻¹ tryptone, 5 g l⁻¹ yeast extract and 5 g l⁻¹ NaCl) was autoclaved and used for the cultivation of *E. coli*.

Peptides with the sequences FWPLHHHGGGS, GPHKHHAGGGS, HNYHHRHGGGS and HMNHHHHGGGS as well as the hexahistidine peptide (HHHHHHGGGS) that served as a reference peptide were purchased and obtained as chemically synthesized trifluoroacetic acid (TFA) salts with a purity of >85 % (PeptideSynthetics, UK and Proteogenix, France). Aliquots of 20 mM stock solutions in MiliQ-water were prepared and stored at -20 °C until use.

2.2. Determination of phage titer

The phage titer was determined in 24-well plates using a modified titration protocol as described in earlier studies (Matys et al., 2020). Briefly, 250 ml of LB agar (2.5 g tryptone, 1.25 g yeast extract, 1.25 g NaCl and 3.75 g agar) was autoclaved and after cooling to 45 °C, 250 µl of IPTG/Xgal stock solution (0.25 g IPTG (isopropyl-β-D-thiogalactopyranoside), 0.2 g Xgal (5-bromo-4-chloro-3-indolyl-β-D-galactopyranoside) in 5 ml DMF (*N,N*-dimethylformamide)) was added. Afterwards, 1 ml of supplemented agar was pipetted into each well of a 24-well plate and stored at 4 °C until use. Phage dilutions were prepared in LB media. Once the *E. coli* reached an optical density of 0.5, 200 µl of culture were mixed with 10 µl of diluted phage and incubated for 5 min at room temperature. Afterwards, 10 µl of infected *E. coli* suspension was pipetted into one well of a pre-warmed 24-well plate. 200 µl of pre-warmed top agar (10 g l⁻¹ tryptone, 5 g l⁻¹ yeast extract, 5 g l⁻¹ NaCl and 7 g l⁻¹ electrophoresis grade agarose) were distributed on top. The plates were incubated overnight at 37 °C. The next day, the infected blue plaques were counted, and the phage concentration was calculated. Phage titers were determined for all relevant fractions of the biopanning procedure and for the single-clone binding tests.

2.3. Biopanning

The standard biopanning procedure provided by NEB was modified as follows. In a first step, 100 µl of plain PureCube 100 NTA agarose solution (50 % v/v) (Biozym Scientific GmbH, Austria) were washed three times with TBST to remove excess ethanol from storage. Then, the phage library was diluted in TBST to reach a final amount of 10¹¹ pfu (plaque forming units). 10 µl of the diluted library were kept for the input phage titration, the rest was incubated with blank NTA-beads for 1 h at 22 °C and 950 rpm to remove any non-specific binding phages. A centrifugation step at 50 × g for 1 min allowed the beads to settle. Afterwards, the supernatant containing the non-binding phage was collected and 10 µl were kept for determination of the input titer for the target biopanning.

For the first round of target biopanning, 100 µl Ni- or Co-NTA bead solution (50 % v/v) (MCLAB, USA) were transferred to a 1.5 ml Eppendorf tube and were washed three times with TBST. Afterwards, the

remaining supernatant from the negative biopanning was added to the metal beads and incubated for 1 h at 22 °C at 950 rpm. Following a centrifugation step at 50 × g for 1 min, the supernatant was removed, and the beads were washed 10 times with TBST. Binding phages were eluted by adding 250 µl of 0.2 M glycine-HCl buffer (pH 2.2) and incubating for 10 min at 22 °C and 950 rpm. After another centrifugation step (50 × g, 1 min), the eluted phages in the supernatant were transferred to a separate 1.5 ml Eppendorf tube and 40 µl of 1 M Tris-HCl buffer (pH 9.1) was added to increase the pH. 10 µl of neutralized phage were kept for phage titration. In the meantime, 20 ml of LB medium supplemented with 20 µg ml⁻¹ were inoculated with one colony of *E. coli* K12 ER2738 and incubated at 37 °C and 200 rpm. Once an optical density between 0.01 and 0.05 was reached, the remaining neutralized target binding phages were added to the culture and amplified for 4.5 h at 37 °C and 200 rpm. After that, the culture was centrifuged for 10 min at 3153 × g at 4 °C. The supernatant was transferred to a fresh tube and after a quick re-spin the upper 80 % were transferred again to a fresh tube. PEG precipitation was performed as described in the standard protocol provided by NEB. After determination of the phage titer of the amplified eluate, the second round of target biopanning was performed as described, keeping the Tween®20 concentration at 0.05 %. For the third round, the Tween®20 concentration in the TBST buffer was increased to 0.1 %. The unamplified eluate from round 3 was titrated onto LB/IPTG/Xgal plates from which plaques could be picked for sequencing. Intermediate amplified phages were stored in 50 % (v/v) glycerol at -20 °C.

For the single clone amplification, an *E. coli* overnight culture was diluted 1:100 in LB media with tetracycline. 1 ml of the diluted culture was distributed to separate wells of a 96-deep well plate. Individual blue plaques were picked from the titration plate and transferred to the culture in the 96-well plate. The plate was then covered with a semi-permeable membrane (Sigma Aldrich, Austria) and incubated at 37 °C for 4.5 h, shaking at 950 rpm. After incubation, the infected cultures were transferred to separate Eppendorf tubes and centrifuged at 20817 × g. DNA extraction from the phage containing supernatant was performed according to the standard NEB protocol. For sequencing, the purified phage DNA was sent to Microsynth GmbH, Austria, where they used the reverse oligonucleotide primer -96 gIII with the sequence 5'-CCCTCATAGTTAGCGTAACG-3'.

2.4. Single phage clone binding assay

To get a first impression about the improved binding properties of selected phage clones, the binding affinity was assessed by evaluating the eluted phage titer (output) compared to the amount of phage used for the metal binding assay (input). The binding ratios of output/input phage were compared to the wildtype phage without any foreign metal-binding peptide on the surface. Hence, the relative binding results of this assay give a first impression on the improved specificity of the binding.

For target binding studies, 300 µl of the corresponding Ni- or Co-NTA bead solution (50 % v/v) were washed three times with 0.1 % TBST buffer. 500 µl of phage clone solution and wildtype phage, diluted with 0.1 % TBST to reach a phage concentration of approximately 10⁹ pfu ml⁻¹, were added to the effective bed volume of 150 µl of beads each. 10 µl of phage solution were kept for the determination of the input phage concentration by titration. The phage/bead mixture was incubated for 1 h at 22 °C and 950 rpm. After one hour, the beads were washed 10 times with 0.1 % TBST buffer followed by elution of the phage particles with 250 µl of glycine-HCl buffer (0.2 M, pH 2.2) for 10 min at 22 °C and 950 rpm. Afterwards, the beads were centrifuged (50 × g for 1 min) to separate the eluted (output) phage particles from the beads. The supernatant was then transferred to a new Eppendorf tube and 40 µl of neutralization buffer (1 M Tris-HCl, pH 9.1) were added. Phage titer of the input and output fraction was determined by titration as previously described. The calculated output/input ratios were normalized to the wildtype binding to the corresponding target material. Experiments

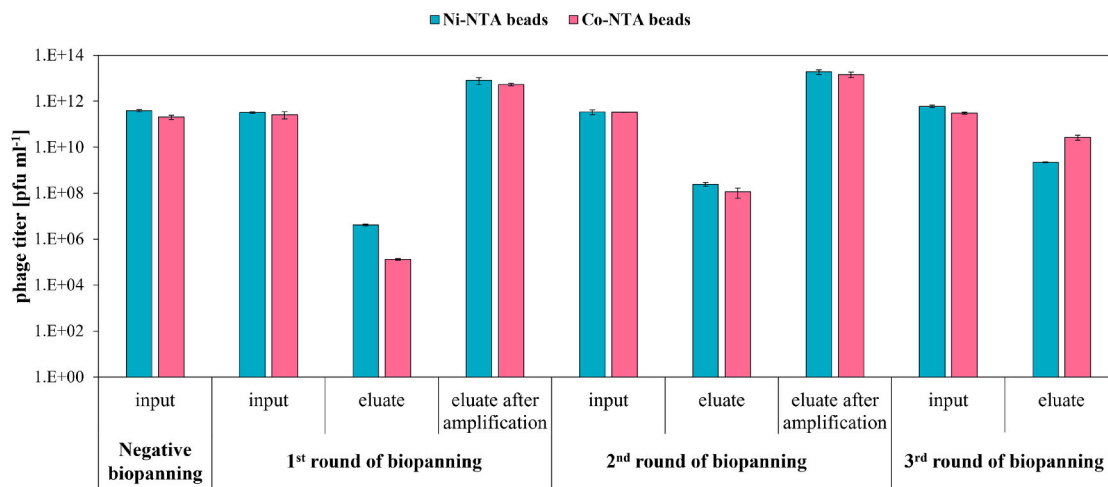


Fig. 1. Screening procedure for nickel- and cobalt-binding peptides by phage surface display with immobilized metal ions. Presented is the phage titer [pfu ml⁻¹] of relevant fractions after each biopanning round as determined by phage titration. Negative biopanning with plain NTA beads was performed to remove unspecific binding phage clones, followed by three rounds of target biopanning using either Ni-NTA beads (turquoise) or Co-NTA beads (pink). Depicted are the input phage titer, the eluate titer after glycine elution and the titer of eluate after the amplification in *E. coli*. Titrations were performed in triplicates. Y-axis is in logarithmic scale for better visualization. (For interpretation of the references to colour in this figure legend, the reader is referred to the web version of this article.)

were performed in triplicates.

2.5. Isothermal titration calorimetry

Isothermal titration calorimetry (ITC) measurements were performed using both the MicroCal PEAQ-ITC and the MicroCal PEAQ-ITC Automated (Malvern Panalytical, UK). The measuring cell contained 200 μ l of the peptide sample between 76 and 234 μ M (see Table 2) and the syringe was filled with 40 μ l either 2 mM NiCl₂ or CoCl₂ solution. All solutions were dissolved in TBS buffer (pH 7.5). The experiments were performed at 25 °C, the reference power was set to 10 μ cal sec⁻¹, and the stirring speed to 750 rpm. After an initial delay of 60 s, the first injection of 0.4 μ l was pipetted into the cell within 0.8 s followed by 18 single injections of 2 μ l within 4 s. Before each subsequent injection, the instrument waited for 150 s. Control experiments for the titration of metal solution into buffer without peptide were performed under the same

conditions and the measured heat of dilution was subtracted from the data of the complex formation. Data was processed with the MicroCal PEAQ-ITC analysis software, version 1.41. Individual titration peaks are integrated and presented in a Wiseman plot. By fitting the resulting isotherm to the one-site binding model, the reaction stoichiometry (N), dissociation constant (K_D) and change in enthalpy (ΔH) can be directly measured. Based on this, the change in free energy (ΔG) and the change in entropy (ΔS) can be calculated according to equations (1) and (2):

$$\Delta G = R \times T \times \ln K \quad (1)$$

$$\Delta G = \Delta H - T\Delta S \quad (2)$$

Table 1

Amino acid sequences of nickel- and cobalt-binding peptides identified by Sanger sequencing from isolated phage clones after three rounds of biopanning. For bioinformatic analysis the TUPScan, Phd7Faster 2.0 and PSBinder tools provided by the program SAROTUP (accessed on the 05.02.2025).

Peptide ID	Sequence							Frequency	Screen no.	Isoelectric point (pI)	Target-unrelated peptide	Propagation advantage	Polystyrene surface-binding
Ni_01	F	W	P	L	H	H	H	12/60	1 and 2	7.02	none	yes	no
Ni_02	G	P	H	K	H	H	A	14/60	1 and 2	8.77	none	no	no
Ni_03	T	S	Y	I	H	H	H	2/60	1	6.73	none	yes	yes
Ni_04	S	G	F	M	M	R	P	1/60	1	9.47	none	no	yes
Ni_05	R	Q	Y	V	E	H	F	1/60	1	6.75	none	no	yes
Ni_06	Y	K	I	P	H	H	H	1/60	1	8.61	none	yes	no
Ni_07	E	H	Y	M	I	T	N	1/60	1	5.24	none	no	yes
Ni_08	M	R	T	Q	P	V	M	1/60	1	9.5	none	yes	no
Ni_09	I	R	F	P	H	H	H	1/60	1	9.77	none	yes	yes
Ni_10	I	Y	V	G	H	H	H	1/60	1	7.02	none	yes	no
Ni_11	V	V	T	R	P	E	L	1/60	1	5.79	none	no	yes
Ni_12	S	P	R	S	H	H	H	1/60	1	9.53	none	yes	no
Ni_13	S	W	K	S	H	H	H	1/60	1	8.53	none	yes	no
Ni_14	S	L	A	G	V	M	P	1/60	1	5.24	none	yes	yes
Ni_15	D	W	Y	H	H	S	V	1/60	2	5.97	none	yes	no
Ni_16	S	M	G	N	S	H	H	1/60	2	6.66	none	no	no
Ni_17	S	G	H	V	S	A	K	1/60	2	8.49	none	yes	no
Ni_18	S	E	Q	H	H	F	H	1/60	2	6.2	none	yes	yes
Ni_19	T	Y	H	H	H	H	D	1/60	2	6.33	suspected	yes	no
Ni_20	N	W	H	H	V	H	H	1/60	2	7.1	none	no	yes
Co_01	H	N	Y	H	H	R	H	17/20	3	8.78	none	no	no
Co_02	H	M	N	H	H	H	H	1/20	3	7.16	suspected	yes	no
Co_03	T	L	W	S	S	S	N	1/20	3	5.19	none	no	no

3. Results and discussion

3.1. Identification of Ni- and Co-binding peptides

To identify selective nickel- and cobalt-binding peptides, subsequent affinity selection steps were conducted. Initially, biopanning was performed with blank NTA beads to remove phage clones nonspecifically binding to the functional groups on the NTA beads other than the metal ions. The non-binding supernatant of this negative biopanning was subsequently used as an input for the first round of target biopanning. Phage titers were determined of all relevant steps from the biopanning (Fig. 1). To keep the input phage concentration always in the same range of approximately 2×10^{11} pfu/ml, amplified phage fractions were diluted accordingly. This approach should aid in the increase of phage clones displaying strong target binding peptides after each round. Similar phage concentrations were achieved with both biopanning procedures, using either Ni- or Co-NTA beads as a target material. After each round of biopanning, the phage titer increased (from 4×10^6 pfu ml⁻¹ in the first nickel biopanning to 2×10^9 pfu ml⁻¹ after the third round and from 1×10^5 pfu ml⁻¹ of the first-round eluate to 3×10^{10} pfu ml⁻¹ for the third-round eluate for cobalt). By keeping the input phage concentration constant, this increase in titer of the eluted phage in subsequent biopanning rounds indicates a successful enrichment of nickel- and cobalt-binding phage clones (Zhang et al., 2019).

After three rounds of biopanning, the amino acid sequences of the heptapeptides from several phage clones were analyzed by Sanger sequencing. For nickel, two independent screening experiments were performed where the experimental setup differed only in the handling of the phage library after the initial negative biopanning. In the first set of experiments, the non-binding supernatant after incubation with plain NTA-beads was amplified before continuing the target biopanning with Ni-NTA beads. In the second screening, the non-binding supernatant was used directly for the incubation with the target material. Hence, an additional amplification step was avoided to exclude amplification induced bias due to faster growing phage clones (Matochko et al., 2014).

In total, 40 individual clones were picked from the first screening for nickel-binding peptides, phage DNA was extracted and sent for sequencing. From the second nickel-screening, 20 phage clones were analyzed. Of these 60 sequences, 1 sequence showed the genotype of M13 KE wildtype and the peptide sequence of 45 positive phage clones was identified. The identified amino acid sequences, their frequencies and isoelectric points are depicted in Table 1. In both independent nickel screenings, 2 phage clones, Ni_01 and Ni_02 with the nickel-binding motifs FWPLHHH and GPHKHHA, were successfully enriched, appearing 12 and 14 times, respectively out of 45 analyzed sequences. One more phage clone, Ni_03 with the nickel-binding motif TSYIHSH, appeared twice in the first screening.

In case of the cobalt biopanning, phage DNA from 20 individual clones was sequenced. Out of these 20 sequences, one sequence was identified as M13 KE wildtype while the other 19 sequences were identified as positive peptide clones. From these 19 sequences, only one clone, Co_01 with the cobalt-binding motif HNYHHRH, was enriched and the sequence appeared 17 times. In all enriched phage clones the most prominent amino acid was histidine. Notably, the histidines appeared more often at the C-terminus of the peptide where it is fused to the pIII phage coat protein. No other common binding motif could be detected. It is also worth mentioning that when performing a biological elution in the nickel biopanning, where the beads after target binding were shortly incubated with *E. coli* cells, as an alternative to the standard glycine elution procedure, totally different sequences were observed after three rounds of biopanning. Additionally, when analyzing the sequenced clones after biological elution with the tools from the BDP database, most of the clones turned out to have polystyrene binding affinities or an increased phage propagation advantage. Hence, glycine elution was used as a standard elution procedure in further biopanning experiments.

From MetalPDB, a database collecting metal-binding sites in biological macromolecular structure from PDB, 3855 and 3492 sequences binding to nickel and cobalt, respectively, can be downloaded (<https://metaldp.cerm.unifi.it/>, accessed on 20.01.2025). The most abundant amino acid in these metal-binding sites is histidine with over 70 % of the nickel-binding sequences and over 40 % of the cobalt-binding sequences containing at least one histidine. This corresponds to the findings in this study where histidine was the most observed amino acid in the newly identified peptide sequences for both metals. This result is not surprising since the ability of histidine to bind to metal ions via the imidazole side chain is well described in literature (Bassan & Marchesan, 2023; Chivers et al., 2024). Hence, this finding proves the feasibility of the biopanning workflow using nickel- and cobalt-ions immobilized on NTA agarose beads as target. It is worth noting that nickel- and cobalt-ions are coordinated by NTA in a tetradentate manner. To fulfill the most common octahedral coordination, two additional interactions are required (Barber-Zucker et al., 2017; Knecht et al., 2009). This means that during the biopanning procedure, the peptides can bind with two sites simultaneously to the immobilized metal ions.

According to the metal-binding sites from MetalPDB, aspartic acid and glutamic acid are also important residues for nickel and cobalt binding. Aspartic acid appeared in 26 % and 19 % in the downloaded nickel- and cobalt-sequences, respectively, followed by glutamic acid with 22 % and 17 % for nickel and cobalt. At physiological conditions, the amino acids glutamic acid and aspartic acid are negatively charged and can therefore contribute to the binding of positively charged metal ions (Matys et al., 2020). Barber-Zucker and coworkers (2017) performed a more detailed binding analysis of different quartets of amino acids to divalent d-block metal cations and report a preference of nickel to bind to more His-containing quartets, such as DHHH and DDHH. Cobalt on the other hand was rather bound to charged quartets with a higher tendency of binding to DEEH and DDEH (Barber-Zucker et al., 2017). In the present study, biopanning was performed at pH 7.5, but both obviously charged amino acids only play a minor role in the newly identified peptides and do not appear in the enriched sequences at all. Cysteines are likewise described in literature to bind to nickel ions with their thiolate groups (Lukács et al., 2021) and were also occurring more often in the metal-binding sites from the MetalPDB database (14 % of the nickel-binding sequences, 4 % of the cobalt-binding sequences). However, cysteines were not present in any of the peptide sequences identified in this study. Previous studies report on the underrepresentation of unpaired cysteine residues in naïve phage libraries. There are four intrinsic cysteine residues in the N1 domain of pIII that could form intramolecular disulfide bonds with an unpaired cysteine residue. This can potentially interfere with the assembly or infection of filamentous phage (Rodi et al., 2002; Sloth et al., 2022). For instance, 'T Hoen and coauthors (2012) sequenced the naïve phage library and described a considerable depletion of cysteine residues to <1 % of all amino acids (Hoen et al., 2012).

In this study, serine was identified as the second most abundant amino acid from the phage display experiments with both metals, however, it did not appear in the significantly enriched sequences (Ni_01, Ni_02 and Co_01). According to the results in Table 1, asparagine at position 2 and 3 seems to play an important role in binding to cobalt. Moreover, valine and proline appeared more often in the nickel-binding sequences, yet, only proline was found in the enriched nickel-sequences at positions 2 and 3. The small amino acids proline and glycine are described in literature as breaking the secondary structure and hence destabilizing proteins. It was shown that one isolated proline can introduce compaction at its position in the sequence (Hazra et al., 2023; Maass et al., 2024). In addition, proline residues can interact with other aromatic residues such as phenylalanine and tryptophan, which are both present in Ni_01, and therefore have an impact on the peptide structure (Imai & Mitaku, 2005).

Compared to earlier biopanning experiments, where sol-gel coated

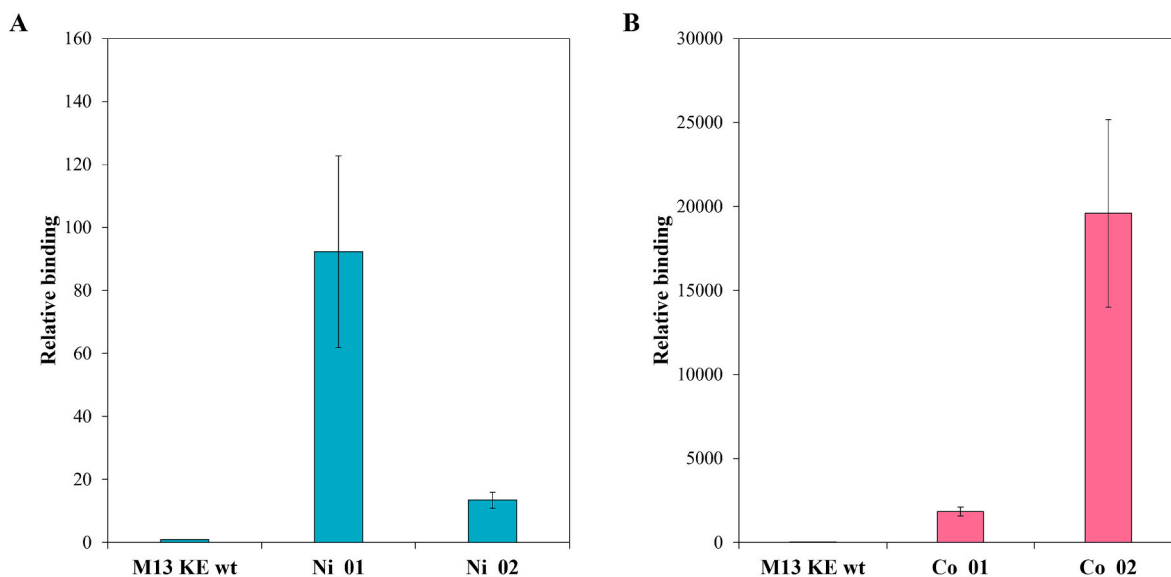


Fig. 2. Binding of selected phage clones to Ni-NTA (A) or Co-NTA (B) agarose beads. Binding of M13 KE wildtype (wt) to the corresponding metal beads was set to 1 and binding of phage clones was normalized to the wildtype binding. Error bars present the standard error out of a minimum of 3 independent experiments.

glass fiber fabrics loaded with nickel- or cobalt-ions instead of the metal-loaded agarose beads were used, totally different peptide sequences were identified in this study. Previously, threonine, serine and alanine were reported as most prominent amino acids for nickel- and cobalt-binding. Besides, histidine was only the fifth most common amino acid in the identified nickel-binding peptides and did not appear at all in the cobalt-binding peptides (Matys et al., 2020). One explanation for that could be that the biopanning was performed at a lower pH of 5.4 compared to pH 7.5 in this study. Histidine, with a pKa of ~ 6.04 was reported to be more dominant in structures with basic pH values, when the side chain is deprotonated (Barber-Zucker et al., 2017). Surprisingly, although no common peptides were identified, the previously identified best nickel-binder shares a common motif KHH with Ni_02. A similar biopanning approach was employed by Li et al. (2019), using Ni-NTA agarose beads as a target material. In contrast to this study, they used the Ph.D.TM-12 peptide library (E8110S, NEB) and eluted with two different imidazole concentrations. They report three enriched peptide clones, but no common motif to the peptides in this study was detected (Li et al., 2019).

Bioinformatic analysis using the SAROTUP tools TUPScan, TUPredict and PhD7faster (<https://i.uestc.edu.cn/sarotup3/index.html>, accessed on the 05.02.2025) revealed essential information about target-unrelated or polystyrene binding properties and clone propagation advantages due to faster growing phages. From the two clones that were enriched during the nickel biopanning, Ni_01 was predicted to have a propagation advantage while Ni_02 seems to be a true nickel-binding peptide. On the other hand, Ni_03 which appeared 2 times in the first screen was predicted to bind to polystyrene and have a propagation advantage. Two peptides (Ni_19 and Co_02) were suspected to bear a known TUP motif, both being confirmed or suspected divalent metal ion binders. Additionally, both phage clones seem to have an additional propagation advantage. Similar peptides to Ni_01, Ni_15 and Ni_19 were identified in the biopanning data bank (BDB) binding to other target materials, although all of them are molecular species as opposed to metal ions. According to the bioinformatic analysis, the one enriched cobalt-clone (Co_01) seems to be a true binder.

Based on this first analysis, two nickel-binding (Ni_01 and Ni_02) and two cobalt-binding phage clones (Co_01 and Co_02) were chosen for further characterization of the binding behavior to the corresponding target metal ion.

3.2. Single-clone characterization

Comparing the output to input ratios in phage binding assays provides valuable information on the binding affinity of the identified phage clones to the target metal ion. In this assay, the specific interaction of phages presenting a newly identified binding sequence on the minor coat protein (pIII) was compared to the non-specific interactions of the wildtype M13 bacteriophage without a foreign peptide on the surface (Winton & Allen, 2023). The binding of the identified phage clones to the metal-loaded agarose beads needs careful consideration because the surface of the M13 phage can offer multiple possible metal-binding sites next to the displayed peptide (Ye et al., 2024). In addition, the three residues of the major pVIII coat protein, Glu2, Asp4 and Asp5, are negatively charged at neutral pH (Lambooy et al., 2009). Hence, unspecific binding from the wildtype M13 phage to the positively charged metal beads was expected. Thorough washing steps assisted in removing those unspecific binders but the wildtype binding to the beads still needed to be accounted for.

Both selected nickel-binding phage clones, Ni_01 and Ni_02, showed a substantial improvement in binding over the wildtype. Ni_01 exhibited a 92.3-fold greater affinity and Ni_02 was binding 13.5 times better to the Ni-NTA beads than the wildtype (Fig. 2). An unpaired *t*-test revealed no significant binding difference between the two clones to the Ni-NTA beads (two-tailed *p*-value = 0.07) but a significant difference in binding of each clone to the beads compared to the wildtype binding (two-tailed *p*-values ≤ 0.05). More striking, the two selected cobalt-binding clones showed an even higher improvement of binding to Co-NTA beads by 1847.1- and 19595.1-fold for Co_1 and Co_2 compared to the wildtype. Here, the difference in binding between the clones to the Co-NTA beads as well as the binding difference of each clone compared to the wildtype binding is significant (two-tailed *p*-values ≤ 0.05). Interestingly, the best nickel-binding peptide from the constrained library (CNAKHHPRC) showed a similar binding affinity to Ni-NTA beads as Ni_02 of approximately 10-fold improvement compared to the wildtype phage (Matys et al., 2020). As previously mentioned, in the cyclic Ph.D.TM-C7C constrained library, the heptapeptides are flanked by two cysteines and therefore represented as a loop on the minor phage coat protein. Ni_02 is a linear peptide and out of 7 amino acids, although having a different order, only two amino acids differ between Ni_02 (GPHKHA) and NAKHHPR. Since the binding of the two phage clones to Ni-NTA beads is similar, it is assumed that the KHH binding motif plays an important role

Table 2

Thermodynamic parameters for the binding of the two nickel- and two cobalt-binding peptides to their respective target metal ion at 2 mM and vice versa. Experiments were performed in triplicates at pH 7.5 and 25 °C. Data was fitted using the one-set-of-sites model.

Peptide ID	c [M]	Metal ion	N	K_D [M]	ΔH [kJ/mol]	ΔG [kJ/mol]	$-\Delta S$ [kJ/mol]
Ni_01	$1.30 \times 10^{-4} \pm 0$	Ni ²⁺	0.90 ± 0.04	$7.29 \times 10^{-5} \pm 9.28 \times 10^{-6}$	-41.17 ± 3.18	-23.67 ± 0.34	17.53 ± 3.50
Ni_01	$1.92 \times 10^{-4} \pm 4.21 \times 10^{-5}$	Co ²⁺	Set to 1	$8.65 \times 10^{-4} \pm 5.14 \times 10^{-5}$	-38.90 ± 7.84	-17.53 ± 0.17	21.43 ± 7.78
Ni_02	$7.60 \times 10^{-5} \pm 1.34 \times 10^{-5}$	Ni ²⁺	1.15 ± 0.21	$2.90 \times 10^{-5} \pm 2.39 \times 10^{-6}$	-28.50 ± 0.62	-25.93 ± 0.21	2.58 ± 0.82
Ni_02	$2.34 \times 10^{-4} \pm 1.18 \times 10^{-5}$	Co ²⁺	Set to 1	$4.01 \times 10^{-4} \pm 5.24 \times 10^{-5}$	-22.23 ± 2.31	-19.40 ± 0.29	2.80 ± 1.97
Co_01	$2.16 \times 10^{-4} \pm 2.73 \times 10^{-5}$	Co ²⁺	0.57 ± 0.08	$1.63 \times 10^{-5} \pm 2.10 \times 10^{-6}$	-44.93 ± 6.50	-27.40 ± 0.29	17.56 ± 6.18
Co_01	$2.17 \times 10^{-4} \pm 2.69 \times 10^{-5}$	Ni ²⁺	0.69 ± 0.10	$5.37 \times 10^{-6} \pm 4.21 \times 10^{-7}$	-60.70 ± 1.50	-30.13 ± 0.21	30.57 ± 1.70
Co_02	$2.11 \times 10^{-4} \pm 1.23 \times 10^{-5}$	Co ²⁺	0.72 ± 0.06	$6.44 \times 10^{-6} \pm 3.45 \times 10^{-7}$	-42.37 ± 7.17	-29.67 ± 0.12	12.70 ± 7.08
Co_02	$2.16 \times 10^{-4} \pm 1.23 \times 10^{-5}$	Ni ²⁺	0.82 ± 0.01	$1.37 \times 10^{-5} \pm 1.55 \times 10^{-6}$	-67.30 ± 1.02	-27.77 ± 0.26	39.53 ± 0.76

in binding to nickel ions.

Moreover, the four N-terminal residues (Asp-Ala-His-Lys) of human serum albumin (HSA) were described as a metal binding site for Ni²⁺ and Co²⁺ having a histidine at position 3 and a lysine at position 4, which is the same in Ni_02. Histidine provides an imidazole nitrogen which together with the N-terminal amino group, two deprotonated backbone amide nitrogens from histidine and alanine and the carboxylate side chain from aspartic acid are involved in the binding to Ni²⁺ and Co²⁺ (Cho et al., 2022). Furthermore, Medici and colleagues (2013) report the importance of histidine in the third position together with lysine at position 4 in the coordination with Ni(II) albeit this effect was only observed in the entire HSA protein and not its 24-amino acid peptide (Medici et al., 2013).

All four selected phage clones showed a superior binding to immobilized metal ions when compared to the wildtype phage. However, in real world applications, the metal ions are in solution and albeit being a powerful screening tool, applying phages for metal recovery is impractical for various reasons. For example, phages might lose their capability to express the recombinant peptide due to mutations in their genome (Lederer et al., 2019). Hence, the metal-binding ability of the peptides themselves without the phage backbone to metal ions in solution was analyzed using isothermal titration calorimetry.

3.3. Binding behavior of free peptides in solution

Metal to peptide titrations were performed using isothermal titration calorimetry (ITC) which revealed thermodynamic information about the metal-peptide interaction. ITC is a powerful technology since it does not require any modifications of the molecules such as labeling or immobilization on a surface. During ITC measurements, the evolution of heat during the titration of aliquots of binding partner in the ITC syringe to the peptide in the sample cell is recorded. From the measured successive reaction heats and the shape of the saturation curve, changes in molar enthalpy and Gibbs free energy, the equilibrium dissociation constant (K_D) and the molar ratio of the reaction can be derived (Brautigam et al., 2016).

For the ITC measurements, experimental parameters were chosen to reflect the environment of the phage display experiments and subsequent single-clone binding tests. Hence, metal solutions and peptide dilutions were prepared in TBS buffer, pH 7.5. For peptide synthesis, a short GGGs-linker was added C-terminal to the peptide sequence to reassemble the immobilization on the phage surface during biopanning. There, the peptides are fused with a short GGGs-linker to the N-terminus of the minor pIII coat protein. The hexahistidine peptide (HHHHHHGGGS) served as a reference peptide. The experimental data was fitted using the MicroCal PEAQ-ITC Software V1.41 (MicroCal-Malvern Pananalytical, Malvern, UK). For all titration experiments, the one-site binding model calculated the best fit (Table 2). Overall, the binding behavior for both metals to all the four peptides was exothermic. The negative Gibbs free energy indicates spontaneous reactions, which implies favorable binding of the metals by the peptides. Negative enthalpy changes as well as positive entropy changes are favorable suggesting that both, the enthalpic and entropic factors, contribute to

the feasibility of the interaction (Xiao et al., 2020).

The fitted titration isotherm for the interaction of nickel with both nickel-binding peptides followed an almost ideal sigmoidal shape in the Wiseman plot (Fig. 3). Hence, the stoichiometry of the metal-peptide complex could be determined as a 1:1 reaction. The binding affinities are in the mid- to lower micromolar range (Table 2), with dissociation constants (K_D) of 72.9 μ M for Ni_01 and 29.0 μ M for Ni_02. In comparison, previous identified nickel-binding peptide (CNAKHHPRCGGG) displayed a dissociation constant of 104 μ M under similar conditions (Matys et al., 2022). While in this latest study no interaction between the nickel-binder and cobalt could be determined, in this study significantly lower binding affinities of the nickel-peptides to cobalt (K_D values of 865 μ M for Ni_01 and 401 μ M for Ni_02) were calculated. The entropic contributions for all binding events are small, especially for the binding of nickel and cobalt to Ni_02, indicating small conformational changes or hydrophobic interactions. It is worth mentioning that the binding of cobalt to both nickel-binding peptides at the present conditions could only be fitted when the binding stoichiometry (N) was fixed at 1. For measurements at low C value, where the ratio of cell concentration to the anticipated dissociation constant is low, fixing the N value may reduce the experimental error. Studies have shown that under a wide range of experimental conditions, fixing N at its nominal value decreases the uncertainty in the binding enthalpy and free energy, especially for low C experiments (Kantonen et al., 2017). Overall, this data suggests that the nickel-binding peptides identified by phage display in this study, Ni_01 and Ni_02, have a 12- and a 14-fold greater affinity to its target ion compared to the binding affinity to cobalt.

Binding of peptides from the N-terminal binding site of HSA to transition metal ions was reported with dissociation constants of 0.15 μ M and 110 μ M for nickel and cobalt at pH 7.4 (Bal et al., 2013). In an additional study, the binding of a dodecapeptide from the N-terminal HSA sequence to cobalt was determined with a K_D of 75 μ M (Cho et al., 2022). Albeit the calculated binding affinity for Ni_02 to cobalt in this study (401 μ M) is about 3–5 times lower, this result strengthens previous findings highlighting the importance of histidine at position 3 and lysine at position 4 for cobalt binding.

In general, both cobalt-binding peptides display higher affinities for nickel than the identified nickel-binding peptides. This can be explained by the higher amount of histidines in both cobalt-binding peptides (4 and 5 histidine residues compared to 3 histidines in Ni_01 and Ni_02) which are known to bind to divalent metal ions. Interestingly, Co_01 with 4 histidines shows a higher binding affinity to Ni²⁺ than to Co²⁺ whereas for Co_02 harboring 5 histidines the binding preference is inverted (Table 2). The distance between the histidines and the impact of other amino acids on the three-dimensional arrangement seems to impact the binding to the metal ions. Earlier studies also describe that the position and surface accessibility of the histidine residues is more important than their absolute number regarding the binding strength to metal ions (Mooney et al., 2011). The binding of the reference hexahistidine peptide to Ni²⁺ and Co²⁺ was measured revealing dissociation constants of 3.9 μ M for Ni²⁺ and 22.6 nM for Co²⁺ under the particular experimental conditions (Table S1 and Fig. S1 in the supplementary data). There is good agreement with reported dissociation constants of

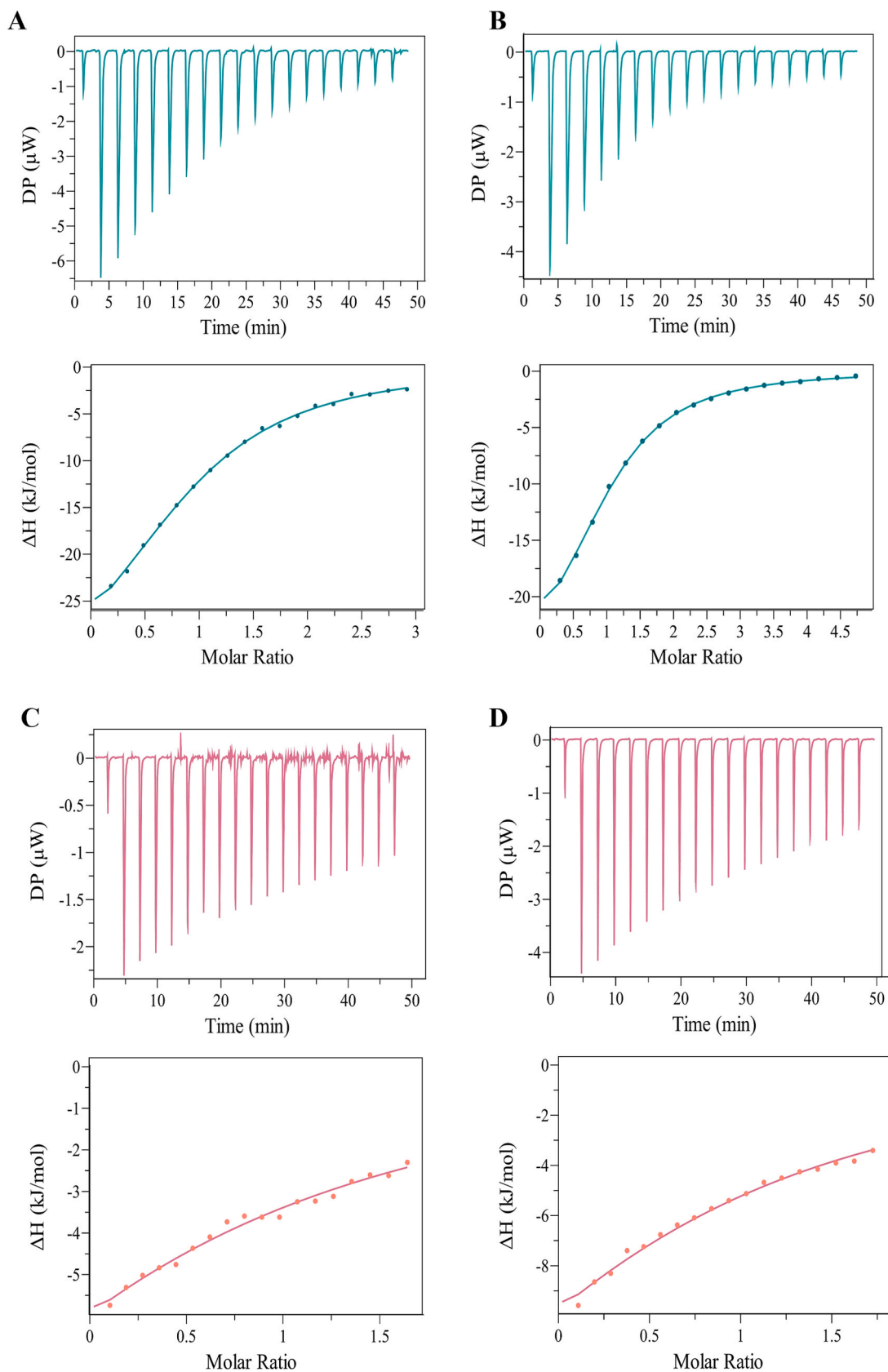


Fig. 3. Isothermal titration calorimetry results of titrating 2 mM of Ni^{2+} to the two novel nickel-binding peptides, Ni_01 (A) and Ni_02 (B), and 2 mM Co^{2+} to Ni_01 (C) and Ni_02 (D). Plotted are the integrated heat peaks [kJ mol^{-1}] against the molar ratio in the lower diagram and the raw data where the heat rate [μW] is plotted against the time [min] in the upper diagram. Data was fitted using the one-set-of-sites model. Measurements were performed in triplicates; one representative measurement is depicted.

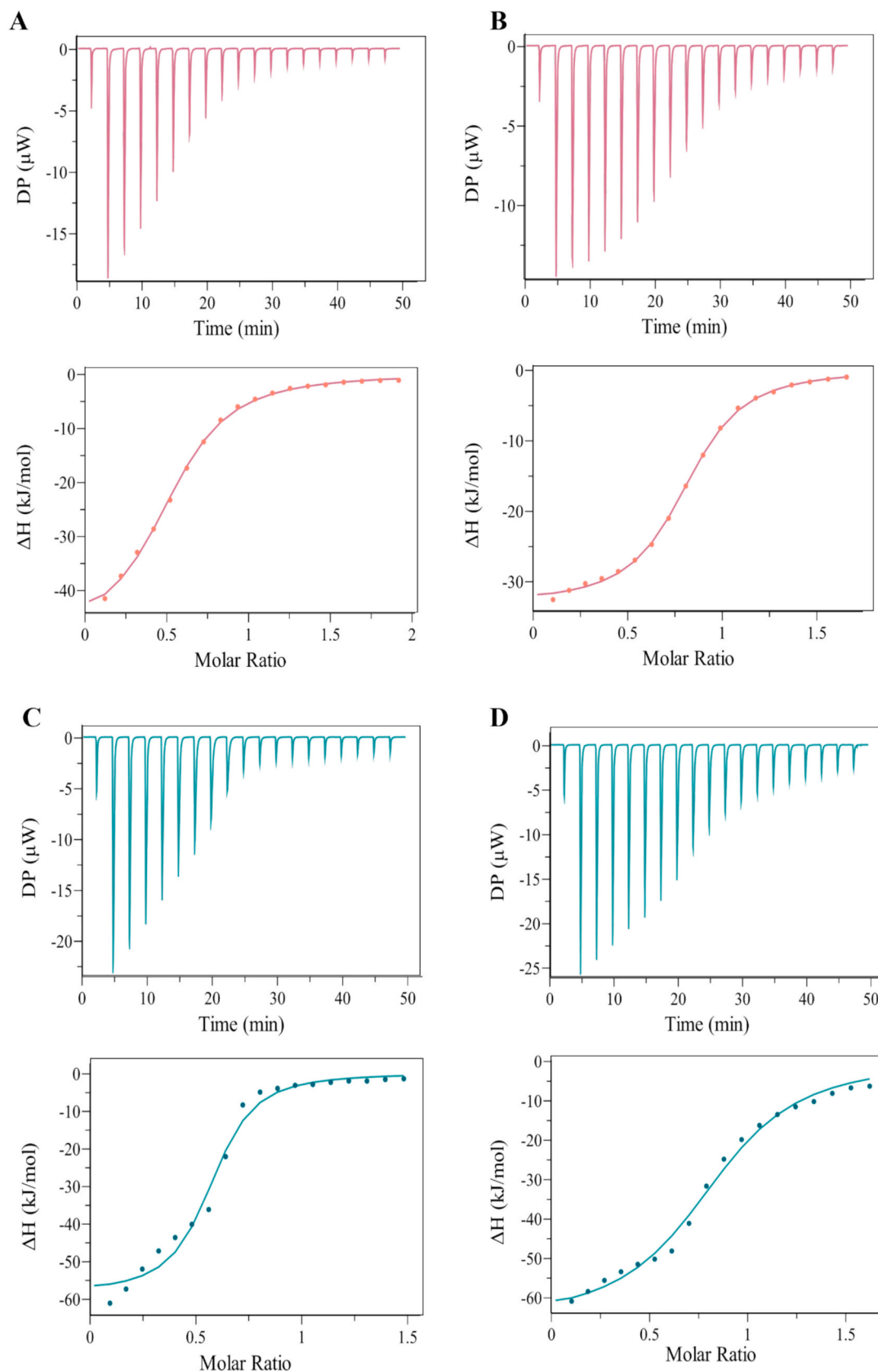


Fig. 4. Isothermal titration calorimetry results of titrating 2 mM of Co^{2+} to the two novel cobalt-binding peptides, Co_01 (A) and Co_02 (B), and 2 mM Ni^{2+} to Co_01 (C) and Co_02 (D). Plotted are the integrated heat peaks [kJ mol^{-1}] against the molar ratio in the lower diagram and the raw data where the heat rate [μW] is plotted against the time [min] in the upper diagram. Data was fitted using the one-set-of-sites model. Measurements were performed in triplicates; one representative measurement is depicted.

approximately 1 μM for hexahistidine-tagged proteins to Ni^{2+} -NTA which is widely used in affinity chromatography. Binding to Co^{2+} is more specific than to Ni^{2+} but comes at the cost of a weaker binding (Knecht et al., 2009; Lingg et al., 2020). The highest binding affinities for the newly identified peptides were measured for the binding of cobalt to Co_02 and nickel to Co_01 with respective K_D values of 6.4 μM and 5.4 μM reflecting the binding affinity of the hexahistidine peptide to Ni^{2+} (Fig. 4 and Table 2). These results are interesting since Co_01 was originally identified in the cobalt biopanning but shows a three-fold higher affinity to nickel according to the ITC results. Generally, it was expected that the peptides identified in this biopanning experiments would bind to both metals to a certain extent since they are quite similar. This phenomenon was already described in previous studies (Matys et al., 2017, 2020). Nevertheless, it was clearly shown within the ITC results that both nickel-binding peptides prefer nickel over cobalt and Co_02 shows a two-fold higher affinity to cobalt compared to nickel.

The newly identified peptides show similar binding affinities to nickel compared to the already established hexahistidine peptide which was used as a reference. These results demonstrate the power of phage surface display technology to identify novel and highly specific metal-binding peptides. The different affinities to nickel and cobalt provide a promising starting point in terms of a potential application for selective metal recovery. ITC experiments were also performed at a lower pH of 3 but no K_D values could be detected because of the weak heat changes which could not be distinguished from the control measurements. These results make sense since for both metal ions, Ni and Co, histidines were suspected to be the main binding sites. At a pH lower than the pK_a of the histidine sidechain of approximately 6.04, the nitrogen of the imidazole side chain is protonated. Binding of metal ions is therefore less likely (Barber-Zucker et al., 2017; Chivers et al., 2024). This clearly indicates that if the peptides should be used for metal recovery from leachate solutions, which usually have a very low pH below 2, further experiments need to focus onto optimization of reaction parameters. Future studies will involve the immobilization of the peptides on a suitable matrix and testing the selectivity of the metal recovery under various conditions. To gain more insights into the binding mechanism of the peptides with their target metal, molecular dynamics simulations could be performed. However, the modelling of metal specificity into proteins or peptides remains challenging due to substantial computational requirements (Urbina et al. 2019).

The potential of peptide-based materials for recovery of metals from aqueous solutions has already been demonstrated in several studies. Schönberger et al. (2021) used gallium-binding peptides immobilized on polystyrene beads in a continuous approach where Ga was removed from wastewaters of a wafer industry, while binding of the peptides to arsenic was minimal (Schönberger et al., 2021). In a different study by Urbina et al. 2019, a copper-binding peptide was used to functionalize fungal mycelia demonstrating the removal of Cu from aqueous metal solutions e.g., from electronic waste (Urbina et al., 2019). Present results of this study suggest a multistep process where nickel could be recovered first by the nickel-binder followed by cobalt recovery from mixed metal waste streams, e.g. from battery recycling. In such a multistep recycling process, other metals such as aluminum and copper could be recovered by selective precipitation in a first step, hence, raising the solution pH to approximately 5–6. The selective precipitation of nickel and cobalt is more challenging, here a peptide-based approach could offer a straightforward and environmentally friendly solution. Peptides can be implemented in conventional recycling processes such as flotation or membrane separation by either linking a hydrophobic tail to the peptidic head or by incorporation of the metal-binding peptides into separation membranes (Lederer & Boelens, 2025). The application of the newly identified nickel- and cobalt-binding peptides to these metal solutions will be investigated in a further study.

4. Conclusion

In this study, two novel nickel- (FWPLHHH and GPHKHHH) and two cobalt-binding peptides (HNYHHRH and HMNHHHH) were identified. By presenting the metal ions on the surface of NTA-beads it was possible to thoroughly screen a combinatorial heptapeptide library and select promising strong binding peptides. All four peptides showed enhanced target metal-binding properties while still bound to the phage backbone. Furthermore, when the binding event was analyzed independently from the phage anchor, both nickel-binding peptides revealed more than 10-fold better affinities to nickel than to cobalt. Both cobalt-binding peptides displayed high affinities for cobalt and nickel, with Co_02 showing a two-fold higher affinity to cobalt and Co_01 showing a three-fold higher affinity to nickel. The results clearly revealed that the peptides have different preferences for the similar metal ions nickel and cobalt. Further investigations will focus on the applicability of these peptides for the selective recovery of nickel and cobalt from mixed metal waste streams, e.g. from spent lithium-ion batteries. In addition, the developed methodology could in future also be applied for the identification of peptides with enhanced binding abilities to different divalent metal ions. Therefore, the successful identification of specifically metal-binding peptides presents a promising first step in the development of a more sustainable and green technology for an efficient separation of highly similar metals from mixed metal waste streams and secondary resources.

CRedit authorship contribution statement

Anna Sieber: Writing – original draft, Visualization, Supervision, Methodology, Formal analysis, Data curation, Conceptualization. **Anastasia Kalampaka:** Methodology, Data curation. **Sabine Matys:** Data curation. **Franziska Lederer:** Writing – review & editing. **Klemens Kremser:** Writing – review & editing, Supervision, Funding acquisition, Conceptualization. **Doris Ribitsch:** Writing – review & editing, Supervision, Funding acquisition. **Georg M. Guebitz:** Writing – review & editing, Supervision.

Funding

The authors gratefully acknowledge the funding support of K1-MET GmbH, the metallurgical competence center. This research received funding from the module FuLiBatter. which is supported by COMET (Competence Center for Excellent Technologies), the Austrian program for competence centers. COMET is funded by the Federal Ministry for Climate Action, Environment, Energy, Mobility, Innovation and Technology, the Federal Ministry for Labour and Economy, the Federal States of Upper Austria and Styria as well as the Styrian Business Promotion Agency (SFG). Furthermore, Upper Austrian Research GmbH continuously supports the module. Besides the public funding from COMET, this research project is partially financed by the company partners Audi, BRAIN Biotech, Ebner Industrieofenbau, RHI Magnesita, Saubermacher, TÜV SÜD Landesgesellschaft Österreich, voestalpine High-Performance Metals, and VTU Engineering and the scientific partners acib, BOKU University, Coventry University, Montanuniversitaet Leoben, and UVR-FIA. Open access funding was provided by the Boku University. Additionally, the Ph.D. project was supported by the Doctoral School “Advanced Biorefineries – Chemistry & Materials” (ABC&M, BOKU).

Declaration of competing interest

The authors declare that they have no known competing financial interests or personal relationships that could have appeared to influence the work reported in this paper.

Acknowledgements

The MicroCal PEAQ-ITC Automated was kindly provided by the

Connective Base GmbH and the project was supported by the BOKU Core Facility Biomolecular & Cellular Analysis (CF BmCA). The MicroCal PEAQ-ITC was kindly provided by the Biotechnology Department at the Helmholtz Institute Freiberg for Resource Technology at the Helmholtz-Zentrum Dresden-Rossendorf (HZDR). Furthermore, the authors wish to thank Georg Schütz from the CF BmCA his valuable assistance with the ITC measurements and data analysis.

Appendix A. Supplementary data

Supplementary data to this article can be found online at <https://doi.org/10.1016/j.wasman.2025.115145>.

Data availability

No data was used for the research described in the article.

References

- Aberdeen, S., Foster, R.I., Choi, S., 2025. Nickel and cobalt separation via speciation using deep eutectic solvent-based ion exchange. *Sep. Purif. Technol.* 375. <https://doi.org/10.1016/j.seppur.2025.133833>.
- Andreini, C., Rosato, A., 2022. Structural bioinformatics and deep learning of metalloproteins: recent advances and applications. *Int. J. Mol. Sci.* Vol. 23, Issue 14, MDPI. <https://doi.org/10.3390/ijms23147684>.
- Bal, W., Sokolowska, M., Kurowska, E., Faller, P., 2013. Binding of transition metal ions to albumin: Sites, affinities and rates. In *Biochimica et Biophysica Acta - General Subjects* 1830 (12), 5444–5455. <https://doi.org/10.1016/j.bbagen.2013.06.018>.
- Barber-Zucker, S., Shaanan, B., Zarivach, R., 2017. Transition metal binding selectivity in proteins and its correlation with the phylogenomic classification of the cation diffusion facilitator protein family. *Sci. Rep.* 7 (1). <https://doi.org/10.1038/s41598-017-16777-5>.
- Bassan, G.A., Marchesan, S., 2023. Peptide-based materials that exploit metal coordination. *Int. J. Molecular Sci.* 24 (1), MDPI. <https://doi.org/10.3390/ijms24010456>.
- Braun, R., Bachmann, S., Schönberger, N., Matys, S., Lederer, F., Pollmann, K., 2018. Peptides as biosorbents – Promising tools for resource recovery. *Res. Microbiol.* 169 (10), 649–658. <https://doi.org/10.1016/j.resmic.2018.06.001>.
- Brautigam, C.A., Zhao, H., Vargas, C., Keller, S., Schuck, P., 2016. Integration and global analysis of isothermal titration calorimetry data for studying macromolecular interactions. *Nat. Protoc.* 11 (5), 882–894. <https://doi.org/10.1038/nprot.2016.044>.
- Chakankar, M., Lederer, F., Jain, R., Matys, S., Kutschke, S., & Pollmann, K. (2024). State-of-the-Art Biotechnological Recycling Processes. In *Management of Electronic Waste* (Issue December, pp. 375–405). Wiley. <https://doi.org/10.1002/9781119894360.ch15>.
- Chen, Z., Li, Z., Chen, J., Kallem, P., Banat, F., & Qiu, H. (2022). Recent advances in selective separation technologies of rare earth elements: a review. In *Journal of Environmental Chemical Engineering* (Vol. 10, Issue 1). Elsevier Ltd. <https://doi.org/10.1016/j.jece.2021.107104>.
- Chivers, P.T., Basak, P., Maroney, M.J., 2024. One his, two his... the emerging roles of histidine in cellular nickel trafficking. *J. Inorg. Biochem.* 259 (April), 112668. <https://doi.org/10.1016/j.jinorgbio.2024.112668>.
- Cho, Y., Mirzapour-Kouhdasht, A., Yun, H., Park, J.H., Min, H.J., Lee, C.W., 2022. Development of Cobalt-binding peptide chelate from human serum albumin: cobalt-binding properties and stability. *Int. J. Mol. Sci.* 23 (2). <https://doi.org/10.3390/ijms23020719>.
- Collins, R. N., & Kinsela, A. S. (2010). The aqueous phase speciation and chemistry of cobalt in terrestrial environments. In *Chemosphere* (Vol. 79, Issue 8, pp. 763–771). Elsevier Ltd. <https://doi.org/10.1016/j.chemosphere.2010.03.003>.
- El Ouardi, Y., Virolainen, S., Massima Mouele, E. S., Laatikainen, M., Repo, E., & Laatikainen, K. (2023). The recent progress of ion exchange for the separation of rare earths from secondary resources – A review. In *Hydrometallurgy* (Vol. 218). Elsevier B.V. <https://doi.org/10.1016/j.hydromet.2023.106047>.
- Fan, E., Li, L., Wang, Z., Lin, J., Huang, Y., Yao, Y., Chen, R., & Wu, F. (2020). Sustainable Recycling Technology for Li-Ion Batteries and Beyond: Challenges and Future Prospects. In *Chemical Reviews* (Vol. 120, Issue 14, pp. 7020–7063). American Chemical Society. <https://doi.org/10.1021/acs.chemrev.9b00535>.
- Hazra, M.K., Gilron, Y., Levy, Y., 2023. Not only expansion: Proline content and density also induce disordered protein conformation compaction. *J. Mol. Biol.* 435 (17). <https://doi.org/10.1016/j.jmb.2023.168196>.
- He, B., Chai, G., Duan, Y., Yan, Z., Qiu, L., Zhang, H., Liu, Z., He, Q., Han, K., Ru, B., Guo, F.B., Ding, H., Lin, H., Wang, X., Rao, N., Zhou, P., Huang, J., 2016. BDB: Biopanning data bank. *Nucleic Acids Res.* 44 (D1), D1127–D1132. <https://doi.org/10.1093/nar/gkv1100>.
- Huang, J., Ru, B., Li, S., Lin, H., Guo, F.B., 2010. SAROTUP: Scanner and reporter of target-unrelated peptides. *J. Biomed. Biotechnol.* 2010. <https://doi.org/10.1155/2010/101932>.
- Huang, J., Ru, B., Zhu, P., Nie, F., Yang, J., Wang, X., Dai, P., Lin, H., Guo, F.B., Rao, N., 2012. MIMO2.0: a mimotope database and beyond. *Nucleic Acids Res.* 40 (D1). <https://doi.org/10.1093/nar/gkr922>.
- Hummel, W., & Curti, E. (2003). Nickel Aqueous Speciation and Solubility at Ambient Conditions: A Thermodynamic Elegy. In *Monatshefte für Chemie* (Vol. 134, Issue 7, pp. 941–973). Springer Wien. <https://doi.org/10.1007/s00706-003-0010-8>.
- Imai, K., Mitaku, S., 2005. Mechanisms of secondary structure breakers in soluble proteins. *Biophysics* 1, 55–65. <https://doi.org/10.2142/biophysics.1.55>.
- Jeong, J., Selvamani, V., Maruthamuthu kannan, M., Arulsamy, K., Hong, S.H., 2024. Application of the surface engineered recombinant Escherichia coli to the industrial battery waste solution for lithium recovery. *J. Ind. Microbiol. Biotechnol.* 51 (April). <https://doi.org/10.1093/jimb/kuae012>.
- Kantonen, S.A., Henriksen, N.M., Gilson, M.K., 2017. Evaluation and minimization of uncertainty in ITC binding measurements: heat error, concentration error, saturation, and stoichiometry. *Biochim. Biophys. Acta Gen. Subj.* 1861 (2), 485–498. <https://doi.org/10.1016/j.bbagen.2016.09.002>.
- Knecht, S., Ricklin, D., Eberle, A.N., Ernst, B., 2009. Oligohis-tags: Mechanisms of binding to Ni²⁺-NTA surfaces. *J. Mol. Recognit.* 22 (4), 270–279. <https://doi.org/10.1002/jmr.941>.
- Lamboy, J.A., Arter, J.A., Knopp, K.A., Der, D., Overstreet, C.M., Palermo, E.F., Urakami, H., Yu, T.B., Tezgel, O., Tew, G.N., Guan, Z., Kuroda, K., Weiss, G.A., 2009. Phage wrapping with cationic polymers eliminates nonspecific binding between M13 phage and high p/ target proteins. *J. Am. Chem. Soc.* 131 (45), 16454–16460. <https://doi.org/10.1021/ja9050873>.
- Lederer, F.L., Boelens, P., 2025. Peptide-based recycling of critical raw materials from electronic waste: the transition towards a circular economy requires novel and environmentally-friendly solutions to increase the recycling rate from discarded electronic devices. *EMBO Rep.* <https://doi.org/10.1038/s44319-025-00449-x>.
- Lederer, F. L., Braun, R., Schöne, L. M., & Pollmann, K. (2019). Identification of peptides as alternative recycling tools via phage surface display – How biology supports Geosciences. *Minerals Engineering*, 132(December 2018), 245–250. <https://doi.org/10.1016/j.mineng.2018.12.010>.
- Lederer, F.L., Curtis, S.B., Bachmann, S., Dunbar, W.S., Macgillivray, R.T.A., 2016. Identification of lanthanum-specific peptides for future recycling of rare earth elements from compact fluorescent lamps. Identification of Lanthanum-Specific Peptides for Future Recycling of Rare Earth Elements from Compact Fluorescent Lamps. <https://doi.org/10.1002/bit.26240/abstract>.
- Leone, L., Fenza, M.D., Esposito, A., Lombardi, A., 2024. Peptides and Metal Ions : A Successful Marriage for Developing Artificial Metalloproteins. February, 1–27. <https://doi.org/10.1002/psc.3606>.
- Li, H., Dong, W., Liu, Y., Zhang, H., Wang, G., 2019. Enhanced biosorption of nickel ions on immobilized surface-engineered yeast using nickel-binding peptides. *Front. Microbiol.* 10 (JUN). <https://doi.org/10.3389/fmicb.2019.01254>.
- Lin, G.Y., Su, Y.C., Huang, Y.L., Hsin, K.Y., 2024. MESPEUS: a database of metal coordination groups in proteins. *Nucleic Acids Res.* 52 (D1), D483–D493. <https://doi.org/10.1093/nar/gkad1009>.
- Lingg, N., Öhlknecht, C., Fischer, A., Mozgovic, M., Scharl, T., Oostenbrink, C., Jungbauer, A., 2020. Proteomics analysis of host cell proteins after immobilized metal affinity chromatography: Influence of ligand and metal ions. *J. Chromatogr. A* 1633, 461649. <https://doi.org/10.1016/j.chroma.2020.461649>.
- Lukács, M., Csilla Pálkás, D., Szunyog, G., Várnagy, K., 2021. Metal binding ability of small peptides containing cysteine residues. *ChemistryOpen* 10 (4), 451–463. <https://doi.org/10.1002/open.202000304>.
- Maass, D., Boelens, P., Bloss, C., Claus, G., Harter, S., Günther, D., Pollmann, K., & Lederer, F. (2024). Identification of yttrium oxide-specific peptides for future recycling of rare earth elements from electronic scrap. *Biotechnology and Bioengineering*, November 2023, 1–10. <https://doi.org/10.1002/bit.28629>.
- Matochko, W.L., Cory Li, S., Tang, S.K.Y., Derda, R., 2014. Prospective identification of parasitic sequences in phage display screens. *Nucleic Acids Res.* 42 (3), 1784–1798. <https://doi.org/10.1093/nar/gkt1104>.
- Matys, S., Lederer, F. L., Schönberger, N., Braun, R., Lehmann, F., Flemming, K., Bachmann, S., Curtis, S. B., Macgillivray, R. T. A., & Pollmann, K. (2017). Phage display - A promising tool for the recovery of valuable metals from primary and secondary resources. *Solid State Phenomena*, 262 SSP, 443–446. <https://doi.org/10.4028/www.scientific.net/SSP.262.443>.
- Matys, S., Morawietz, L.M., Lederer, F., Pollmann, K., 2022. Characterization of the binding behavior of specific cobalt and nickel ion-binding peptides identified by phage surface display. *Separations* 9 (11). <https://doi.org/10.3390/separations9110354>.
- Matys, S., Schönberger, N., Lederer, F.L., Pollmann, K., 2020. Characterization of specifically metal-binding phage clones for selective recovery of cobalt and nickel. *J. Environ. Chem. Eng.* 8 (2), 103606. <https://doi.org/10.1016/j.jece.2019.103606>.
- Medici, S., Peana, M., Nurchi, V.M., Zoroddu, M.A., 2013. The involvement of amino acid side chains in shielding the nickel coordination site: an NMR study. *In Molecules*. 18 (10), 12396–12414. <https://doi.org/10.3390/molecules181012396>.
- Mooney, J.T., Fredericks, D., Hearn, M.T.W., 2011. Use of phage display methods to identify heptapeptide sequences for use as affinity purification “tags” with novel chelating ligands in immobilized metal ion affinity chromatography. *J. Chromatogr. A* 1218 (1), 92–99. <https://doi.org/10.1016/j.chroma.2010.10.113>.
- Pommeret, A., Ricci, F., Schubert, K., 2022. Critical raw materials for the energy transition. *Eur. Econ. Rev.* 141. <https://doi.org/10.1016/j.eurocorev.2021.103991>.
- Rodi, D.J., Soares, A.S., Makowski, L., 2002. Quantitative assessment of peptide sequence diversity in M13 combinatorial peptide phage display libraries. *J. Mol. Biol.* 322 (5), 1039–1052. [https://doi.org/10.1016/S0022-2836\(02\)00844-6](https://doi.org/10.1016/S0022-2836(02)00844-6).
- Schaeffer, N., Passos, H., Gras, M., Rodriguez Vargas, S.J., Neves, M.C., Svecova, L., Papaiconomou, N., Coutinho, J.A.P., 2020. Selective separation of manganese,

- cobalt, and nickel in a fully aqueous system. *ACS Sustain. Chem. Eng.* 8 (32), 12260–12269. <https://doi.org/10.1021/acssuschemeng.0c04043>.
- Schönberger, N., Braun, R., Matys, S., Lederer, F.L., Lehmann, F., Flemming, K., Pollmann, K., 2019. Chromatopanning for the identification of gallium binding peptides. *J. Chromatogr. A* 1600, 158–166. <https://doi.org/10.1016/j.chroma.2019.04.037>.
- Schönberger, N., Taylor, C., Schrader, M., Drobot, B., Matys, S., Lederer, F.L., Pollmann, K., 2021. Gallium-binding peptides as a tool for the sustainable treatment of industrial waste streams. *J. Hazard. Mater.* 414. <https://doi.org/10.1016/j.jhazmat.2021.125366>.
- Selvamani, V., Jeong, J., Maruthamuthu, M.K., Arulsamy, K., Na, J.G., Hong, S.H., 2023. Construction of the lithium binding peptide displayed recombinant *Escherichia coli* for the specific lithium removal from various metal polluted wastewater. *J. Environ. Chem. Eng.* 11 (1), 109029. <https://doi.org/10.1016/j.jece.2022.109029>.
- Sieber, A., Spiess, S., Rassy, W. Y., Schild, D., Rieß, T., Singh, S., Jain, R., Schönberger, N., Lederer, F., Kremser, K., & Guebitz, G. M. (2024). Fundamentals of bio-based technologies for selective metal recovery from bio-leachates and liquid waste streams. In *Frontiers in Bioengineering and Biotechnology* (Vol. 12). Frontiers Media SA. <https://doi.org/10.3389/fbioe.2024.1528992>.
- Sloth, A.B., Bakhshinejad, B., Jensen, M., Stavnsbjerg, C., Liisberg, M.B., Rossing, M., Kjaer, A., 2022. Analysis of compositional bias in a commercial phage display peptide library by next-generation sequencing. *Viruses* 14 (11). <https://doi.org/10.3390/v14112402>.
- Sole, K. C. (2018). *The Evolution of Cobalt–Nickel Separation and Purification Technologies: Fifty Years of Solvent Extraction and Ion Exchange* (pp. 1167–1191). https://doi.org/10.1007/978-3-319-95022-8_95.
- Sosnowska, M., Łęga, T., Olszewski, M., Gromadzka, B., 2025. Phage display technology in ecotoxicology : phage display derived unique peptide for copper identification in aquatic samples. *Microb. Cell Fact.* <https://doi.org/10.1186/s12934-024-02553-4>.
- T Hoen, P. A. C., Jirka, S. M. G., Ten Broeke, B. R., Schultes, E. A., Aguilera, B., Pang, K. H., Heemskerck, H., Aartsma-Rus, A., Van Ommen, G. J., & Den Dunnen, J. T. (2012). Phage display screening without repetitious selection rounds. *Analytical Biochemistry*, 421(2), 622–631. <https://doi.org/10.1016/j.ab.2011.11.005>.
- Techert, G., Drobot, B., Braun, R., Bloss, C., Schönberger, N., Matys, S., Pollmann, K., Lederer, F.L., 2025. Application of phage surface display for the identification of Eu3 + -binding peptides. *Front. Bioeng. Biotechnol.* 13. <https://doi.org/10.3389/fbioe.2025.1508018>.
- Thota, V., Puddu, V., Perry, C.C., 2024. Phage Display Panning on Silica: Optimization of Elution Conditions for Selection of Strong Binders. <https://doi.org/10.1021/acs.langmuir.4c01108>.
- Urbina, J., Patil, A., Fujishima, K., Paulino-Lima, I.G., Saltikov, C., Rothschild, L.J., 2019. A new approach to biomining: Bioengineering surfaces for metal recovery from aqueous solutions. *Sci. Rep.* 9 (1). <https://doi.org/10.1038/s41598-019-52778-2>.
- Winton, A.J., Allen, M.A., 2023. Rational Design of a Bifunctional Peptide Exhibiting Lithium Titanate Oxide and Carbon Nanotube Affinities for Lithium-Ion Battery Applications. <https://doi.org/10.1021/acscami.2c18018>.
- Xiao, C.Q., Huang, Q., Zhang, Y., Zhang, H.Q., Lai, L., 2020. Binding thermodynamics of divalent metal ions to several biological buffers. *Thermochim Acta* 691 (July), 178721. <https://doi.org/10.1016/j.tca.2020.178721>.
- Yang, T., Zhang, X.Y., Zhang, X.X., Chen, M.L., Wang, J.H., 2015. Chromium(III) Binding Phage Screening for the Selective Adsorption of Cr(III) and Chromium Speciation. *ACS Appl. Mater. Interfaces* 7 (38), 21287–21294. <https://doi.org/10.1021/acscami.5b05606>.
- Ye, Q., Wang, D., & Wei, N. (2024). Engineering biomaterials for the recovery of rare earth elements. In *Trends in Biotechnology* (Vol. 42, Issue 5, pp. 575–590). Elsevier Ltd. <https://doi.org/10.1016/j.tibtech.2023.10.011>.
- Zhang, X., Zhong, M., Zhao, P., Zhang, X., Li, Y., Wang, X., Sun, J., Lan, W., Sun, H., Wang, Z., Gao, H., 2019. Screening a specific Zn(ii)-binding peptide for improving the cognitive decline of Alzheimer’s disease in APP/PS1 transgenic mice by inhibiting Zn2+ -mediated amyloid protein aggregation and neurotoxicity. *Biomater. Sci.* 7 (12), 5197–5210. <https://doi.org/10.1039/c9bm00676a>.